Scientific
Research
Publishing

Fractional Quantum Hall States for Filling Factors 2/3 < ν < 2

Shosuke Sasaki

Center for Advanced High Magnetic Field Science, Graduate School of Science, Osaka University, Osaka, Japan
Email: sasaki@mag.ahmf.sci.osaka-u.ac.jp, zazensou@gmail.com

Abstract

Fractional quantum Hall effect (FQHE) is investigated by employing normal electrons and the fundamental Hamiltonian without any quasi particle. There are various kinds of electron configurations in the Landau orbitals. Therein only one configuration has the minimum energy for the sum of the Landau energy, classical Coulomb energy and Zeeman energy at any fractional filling factor. When the strong magnetic field is applied to be upward, the Zeeman energy of down-spin is lower than that of up-spin for electrons. So, all the Landau orbitals in the lowest level are occupied by the electrons with down-spin in a strong magnetic field at $1 < \nu < 2$. On the other hand, the Landau orbitals are partially occupied by up-spins. Two electrons with up-spin placed in the nearest orbitals can transfer to all the empty orbitals of up-spin at the specific filling factors $\nu_0 = (3j-1)/(2j-1)$, $(4j+1)/(2j+1)$ and so on. When the filling factor ν deviates from ν_0, the number of allowed transitions decreases abruptly in comparison with that at ν_0. This mechanism creates the energy gaps at ν_0. These energy gaps yield the fractional quantum Hall effect. We compare the present theory with the composite fermion theory in the region of $2/3 < \nu < 2$.

1. Introduction

The composite fermion theory introduces a quasi-particle named composite fermion which is an electron bound by even number $2p$ of flux quanta. The theory explains the fractional quantum Hall effect (FQHE) to be the integer quantum Hall effect (IQHE) of the composite fermions with an integer filling factor n. Then the filling factor of electrons becomes $\nu = n/(2pn \pm 1)$ [1]-[12]. The case of $n = 1$ and $p = 1$ yields $\nu = 1/3$ and $\nu = 1$.

The other cases give the electron filling-factors $v \le 2/3$. Thus the original composite fermion theory cannot explain the fractional quantum Hall states with $v > 2/3$. In order to remove this difficulty, an extended theory has been considered as follows:

1) At the filling factor $v > 1$, the IQHE of composite fermions are combined with the IQHE of electrons. Even number of the flux quanta attach to some electrons and the other electrons are not bound by flux quanta. The former electrons are affected by the effective magnetic field and the latter by the applied magnetic field.

2) In the region of $2/3 < v < 1$ even number of flux quanta attach to a hole. Therein the electrons are not bound by flux quanta.

3) The effective magnetic field is anti-parallel to the applied magnetic field at $v = n/(2pn-1)$. So the polarization of electron at $v = n/(2pn-1)$ is opposite to that at $v = n/(2pn+1)$.

Thus the direction of the effective field, the kind of particle (hole or electron) and the number of attached flux quanta are assumed to change with variation of the filling factor. This changing is very artificial. There is another investigation considered by Tao and Thouless [13] [14]. They investigated the FQH states where the Landau orbitals in the lowest level are partially filled with electrons.

We have improved the Tao-Thouless theory on the basis of the fundamental method. There are many configurations of electrons in the Landau orbitals. The sum of the Landau energy, classical Coulomb energy and Zeeman energy takes the minimum value at only one configuration of electrons for any fractional filling factor. In the configuration the nearest electron pairs can transfer to all the empty orbitals for the specific filling factors.

We consider the 2D electron system under a low temperature and a strong magnetic field throughout the present article. When the direction of the magnetic field is upward, the Zeeman energy of down-spin is lower than that of up-spin for electrons. So, in the region $1 < v < 2$ all the Landau orbitals in the lowest level are occupied by the electrons with down-spin. On the other hand the Landau orbitals are partially occupied by up-spins. (Note: In the previous papers [15]-[19] we have already examined the case of a weak magnetic field. In the case both down- and up-spin-electrons partially occupy the lowest Landau orbitals. This special case appears in a weak magnetic field by adjusting the gate voltage. In this paper we investigate only the case of a strong magnetic field.) The up-spin electron pair placed in the nearest orbitals can transfer to all the empty orbitals of up-spin at $v_0 = (4j+1)/(2j+1)$, $v_0 = (3j-1)/(2j-1)$ and so on. When the filling factor v deviates from v_0, the number of allowed transitions decrease abruptly in comparison with that at v_0. This mechanism creates the energy gaps at $v_0 = (3j+1)/(2j+1)$, $(3j-1)/(2j-1)$, $(4j+1)/(2j+1)$, $(2j+2)/(2j+1)$ and so on. These energy gaps can explain the fractional quantum Hall effect in the region $1 < v < 2$ as clarified in the following sections. (We have already succeeded to obtain the energy gaps for the specific filling factors in the regions $v < 1$ and $v > 2$ in the previous articles [20]-[30].)

2. The Fundamental Properties of a Quasi-2D Electron System

Figure 1 shows a quantum Hall device where the electric current flows along the *x*-axis and the Hall voltage appears along the *y*-axis. Therein the magnetic field is applied in the *z*-direction.

The narrow potential $W(z)$ along the *z*-direction is expressed in **Figure 2**. Also **Figure 3** shows the potential $U(y)$ of the *y*-direction. Therein the voltage $V_2 - V_1$ is not zero because the confinement of Hall resistance is realized under a nonzero value of $V_2 - V_1$. The value of the Hall voltage is extremely larger than the potential voltage in the FQHE. So we cannot employ the *x* - *y* symmetry. Also we should take the potential $U(y)$ into consideration.
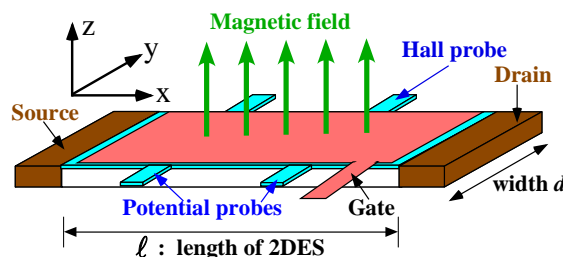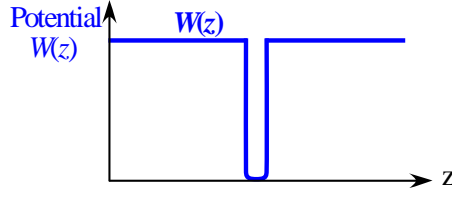

Figure 1. Quantum Hall device.
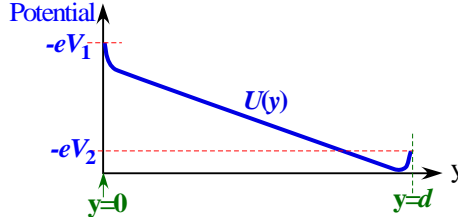
Figure 2. Potential $W(z)$ in the z-direction.

Figure 3. Potential $U(y)$ in the y-direction.

The vector potential, $\mathbf{A}$, has the components,

$$\mathbf{A} = (-yB, 0, 0) \tag{1}$$

where B is the strength of the magnetic field. (Here we cannot use the symmetric vector potential because of the potential $U(y)$.) We express the single electron Hamiltonian, H_0, in the absence of the Coulomb interaction between electrons as,

$$H_0 = \frac{(\mathbf{p} + e\mathbf{A})^2}{2m^*} + U(y) + W(z) + \mu_B g^* s_z B \tag{2}$$

where $U(y)$ and $W(z)$ indicate the potentials confining electrons to an ultra-thin conducting layer. Therein m^* is an effective mass of electron and $\mathbf{p} = (p_x, p_y, p_z)$ is the electron momentum. The last term of Equation (2) indicates the Zeeman energy where g^* is the effective g-factor, μ_B is the Bohr magneton $(\mu_B = \hbar e/(2m))$ and s_z is the z-component of electron spin operator as,

$$s_z = \begin{pmatrix} 1/2 & 0 \\ 0 & -1/2 \end{pmatrix} \tag{3}$$

The potential along the x-axis doesn't exist in the Hamiltonian H_0. (The impurity effect is ignored.) Therefore the eigen-states along the direction x is the plain wave. Then the Landau wave function of the single-electron is given by

$$\psi_{L,J}(x, y, z, s_z) = \sqrt{\frac{1}{\ell}} \exp(ipx/\hbar) u_L H_L\left(\sqrt{\frac{m^*\omega}{\hbar}}(y - \alpha_J)\right) \exp\left(-\frac{m^*\omega}{2\hbar}(y - \alpha_J)^2\right) \phi(z) \chi(s_z) \tag{4a}$$

$$\omega = eB/m^* \tag{4b}$$

$$p = [2\pi\hbar/\ell] \times J \tag{4c}$$

$$\alpha_J = p/(eB) = [2\pi\hbar/(\ell eB)] J \tag{4d}$$

where $\phi(z)$ is the wave function of the ground state along the z-direction, H_L is the Hermite polynomial of L-th degree, u_L is the normalization constant and ℓ is the length of a quasi-2D electron system as shown in **Figure 1**. The integer L is called Landau level number hereafter. The momentum p of the x-direction satisfies the periodic boundary condition, and is related to the value α_J as in Equation (4d). The eigen-energy is

given by

$$E_{L,J,s_z} = \lambda + U(\alpha_J) + (\hbar eB/m^*)\left(L + \frac{1}{2}\right) + \mu_B g^* s_z B, \quad (L = 0,1,2,3,\cdots) \tag{5}$$

where λ is the ground state energy along the z-direction and $U(\alpha_J)$ is the potential energy in the y-direction. The energy difference between two Zeeman levels is equal to $g^*(\hbar eB/(2m))$. Here the effective g-factor for GaAs is about 0.22 times the g-factor of electron in vacuum, namely, $g^* \approx 0.44$. The effective mass m^* for GaAs is 0.067 times the electron mass m in vacuum. Therefore the energy difference between L and $L+1$ Landau levels is about 67 times the Zeeman split energy for GaAs.

Many investigations of the FQHE have used the symmetric property between the x and y directions. However all the actual experiments have carried out in a nonzero voltage $V_2 - V_1$. Accordingly the potential $U(y)$ cannot be ignored.

If we take the other types of the vector potential as

$$\mathbf{A}' = \left(-\frac{1}{2}yB, \frac{1}{2}xB, 0\right), \quad \mathbf{A}'' = (0, xB, 0) \tag{6}$$

the eigen-function in the y-direction is not a plain wave because of the y-dependence of $U(y)$. Consequently the actual quantum Hall system has no $x-y$ symmetry.

Our treatment takes the potential $U(y)$ into consideration which is the appropriate treatment in an actual system. In a many-electron system the total Hamiltonian is given by the following equation as

$$H_T = \sum_{i=1}^{N} H_{0,i} + \sum_{i=1}^{N-1}\sum_{j>i}^{N} \frac{e^2}{4\pi\varepsilon\sqrt{(x_i - x_j)^2 + (y_i - y_j)^2 + (z_i - z_j)^2}} \tag{7}$$

where N is the total number of electrons, ε is the permittivity and $H_{0,i}$ is the single particle Hamiltonian of the i-th electron without the Coulomb interaction as,

$$H_{0,i} = \frac{(\mathbf{p}_i + e\mathbf{A})^2}{2m^*} + U(y_i) + W(z_i) + \mu_B g^* s_i^z B \tag{8}$$

where s_i^z indicates the z-component of the spin for the i-th electron.

The many-electron state is characterized by a set of Landau level numbers $L_1, L_2, \cdots, L_N$, a set of momenta $p_1, p_2, \cdots, p_N$ and spins $s_1^z, s_2^z, \cdots, s_N^z$. The complete set is composed of the Slater determinant as

$$\Psi(L_1,\cdots,L_N;p_1,\cdots,p_N;s_1^z,\cdots,s_N^z) = \frac{1}{\sqrt{N!}} \begin{vmatrix} \psi_{L_1,p_1,s_1^z}(x_1,y_1,z_1) & \cdots & \psi_{L_1,p_1,s_1^z}(x_N,y_N,z_N) \\ \vdots & & \vdots \\ \psi_{L_N,p_N,s_N^z}(x_1,y_1,z_1) & \cdots & \psi_{L_N,p_N,s_N^z}(x_N,y_N,z_N) \end{vmatrix} \tag{9}$$

These states are the eigen-state of $\sum_{i=1}^{N} H_{0,i}$. The expectation value of the total Hamiltonian is expressed by $W(L_1,\cdots,L_N;p_1,\cdots,p_N;s_1^z,\cdots,s_N^z)$ which is given as:

$$W(L_1,\cdots,L_N;p_1,\cdots,p_N;s_1^z,\cdots,s_N^z) = \sum_{i=1}^{N} E_{L_i}(p_i,s_i^z) + C(L_1,\cdots,L_N;p_1,\cdots,p_N) \tag{10}$$

where C is the expectation value of the Coulomb interaction as follows:

$$C(L_1,\cdots,L_N;p_1,\cdots,p_N) = \int\cdots\int \Psi(L_1,\cdots,L_N;p_1,\cdots,p_N)^* \times \sum_{i=1}^{N-1}\sum_{j>i}^{N} \frac{e^2}{4\pi\varepsilon\sqrt{(x_i - x_j)^2 + (y_i - y_j)^2 + (z_i - z_j)^2}} \tag{11}$$

$$\times \Psi(L_1,\cdots,L_N;p_1,\cdots,p_N)\, \mathrm{d}x_1\mathrm{d}y_1\mathrm{d}z_1\cdots\mathrm{d}x_N\mathrm{d}y_N\mathrm{d}z_N$$

Hereafter we call $C(L_1, \cdots, L_N; p_1, \cdots, p_N)$ "classical Coulomb energy". Using the expectation value W, we can divide the total Hamiltonian H_T into the two parts H_D and H_I as follows:

$$H_D = \sum_{L_1, \cdots, L_N} \sum_{p_1, \cdots, p_N} |\Psi(L_1 \cdots L_N; p_1, \cdots, p_N)) W(L_1 \cdots L_N; p_1, \cdots, p_N) \langle \Psi(L_1 \cdots L_N; p_1, \cdots, p_N)| \tag{12a}$$

$$H_I = H_T - H_D \tag{12b}$$

where H_I is composed of the off-diagonal elements only. Accordingly the total Hamiltonian H_T of the quasi-2D electron system is a sum of H_D and H_I as

$$H_T = H_D + H_I \tag{13}$$

Because the Coulomb interaction depends only upon the relative coordinate of electrons, the total momentum along the x-direction conserves in the quasi-2D electron system. That is to say the sum of the initial momenta p_i and p_j is equal to that of the final momenta p_i' and p_j':

$$p_i' + p_j' = p_i + p_j \tag{14}$$

We study the configuration of electrons in the Landau orbitals. The most uniform configuration of electrons is uniquely determined for any filling factor except at the both boundaries. The boundary effects can be neglected in a macroscopic system.

As seen in Equation (8), the $s_z = -1/2$ state has an energy lower than the $s_z = 1/2$ state for $B > 0$. Therefore at $1 < \nu < 2$ all the Landau orbitals with $L = 0$ are occupied by electrons with down-spin and the orbitals are partially occupied by electrons with up-spin in a strong magnetic field and a low temperature. We introduce the total number M of the $L = 0$ orbitals and also express the number of electrons with down-spin and up-spin by $N_\downarrow$ and $N_\uparrow$ respectively. Then we get the following relations in $1 < \nu < 2$ as

$$N_\downarrow = M \tag{15a}$$

$$N_\uparrow < M \tag{15b}$$

$$N = N_\downarrow + N_\uparrow \tag{15c}$$

$$\nu = (N_\downarrow + N_\uparrow)/M \tag{15d}$$

The most uniform configurations will be examined for the case of $3/2 < \nu < 2$ in Section 3 and for $1 < \nu < 3/2$ in Section 4.

3. Electron Configurations and Energy Gaps for $2/3 < \nu < 2$

As an example we examine the FQH state with $\nu = 5/3$. Equation (15d) becomes

$$\nu = 1 + N_\uparrow/M = 5/3$$

This relation gives

$$N_\uparrow/M = 2/3 \tag{16}$$

Then the most uniform configuration of up-spin electrons is the repeat of (filled, empty, filled) for $\nu = 5/3$. **Figure 4** shows the electron configuration in a 3D view where the x, y, z axes are drawn in the upper-left of the figure. Therein the tilted lines with the x-direction express the Landau orbitals of the lowest level schematically. All the orbitals are filled with down-spin electrons for a strong magnetic field because of the Zeeman energy. The up-spin electrons occupy the red-coloured orbitals. The empty orbitals for up-spin are drawn by dashed blue lines in **Figure 4**. This electron configuration of up-spin has the minimum value for the classical Coulomb energy.

We examine the quantum transitions via the Coulomb interaction H_I. All the Coulomb transitions satisfy the momentum conservation along the x-axis. **Figure 4** shows the quantum transitions from the electron pair AB

with up-spin. The momenta at A and B are expressed by p_A and p_B respectively. The momenta p_A and p_B change to p'_A and p'_B after the transition. The momentum conservation gives the following relations as

$$p'_A = p_A - \Delta p \tag{17a}$$

$$p'_B = p_B + \Delta p \tag{17b}$$

where Δp is the momentum transfer. All the allowed transitions are illustrated by the blue allow-pairs in **Figure 4**. Accordingly the transfer momentum takes the following value:

$$\Delta p = (2\pi\hbar/\ell) \times (3n+1), \quad n = 0, \pm1, \pm2, \pm3, \pm4, \cdots \tag{18}$$

We introduce the following summation Z.

$$Z = -\sum_{\Delta p \neq 0, -2\pi\hbar/\ell} \frac{\langle L=0, p_A, p_B | H_I | L=0, p'_A, p'_B \rangle \langle L=0, p'_A, p'_B | H_I | L=0, p_A, p_B \rangle}{W_G - W_{\text{excite}}(p_A \to p'_A, p_B \to p'_B)} \tag{19a}$$

$$p_A = p_B + 2\pi\hbar/\ell \tag{19b}$$

$$p'_A = p_A - \Delta p, \quad p'_B = p_B + \Delta p \tag{19c}$$

Therein the summation is carried out for all the values $\Delta p = (2\pi\hbar/\ell) \times \text{integer}$ except $\Delta p = 0$ and $-2\pi\hbar/\ell$. The elimination comes from disappearance of the diagonal matrix element of H_I. The summation Z is positive, because the denominator in Equation (19a) is negative.

As shown in **Figure 4**, the transfer-momenta from AB (up-spin electron-pair) satisfies Equation (18). Then the number of the transfer-momenta is 1/3 of the total orbitals. Accordingly the perturbation energy ς_{AB} of the pair AB is expressed by using Z as follows;

$$\varsigma_{AB} = -(1/3)Z \quad \text{at} \quad \nu = 5/3 \tag{20}$$

because the momentum-interval, $2\pi\hbar/\ell$, is extremely small in a macroscopic size of a quantum Hall device. The total number of the nearest electron pairs with up-spin is 1/2 of $N_\uparrow$. Therefore we obtain the nearest pair energy per up-spin-electron $\varepsilon_\uparrow$ as

$$\varepsilon_\uparrow = \left(\varsigma_{AB} \times \frac{1}{2} N_\uparrow \right) \Big/ N_\uparrow = -(1/6)Z \quad \text{at} \quad \nu = 5/3 \tag{21}$$

When the filling factor deviates from $\nu = 5/3$, the electron configuration at $\nu \neq 5/3$ changes from the regular repeating of (filled, empty, filled). Accordingly the number of the Coulomb transitions decreases abruptly because the changing disturbs the Coulomb transitions. As an example, the $\nu = 42/25$ state is illustrated in **Figure 5** where the nearest orbitals with up-spin are indicated by red and brown colours.
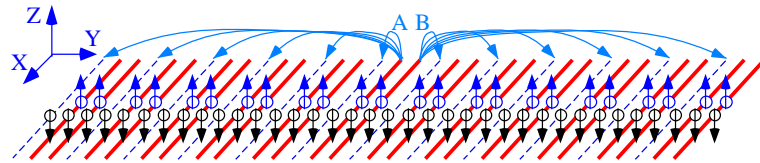

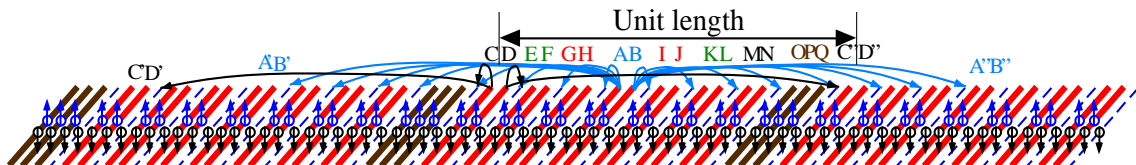**Figure 4.** Electron configuration at $\nu = 5/3$.

Figure 5. Electron configuration at $\nu = 42/25$.

There are 9 nearest electron pairs, namely, AB, CD, EF, GH, IJ, KL, MN, OP and PQ in every unit sequence. The pair CD can transfer to two orbital pairs per unit length as shown by black arrow pairs. Accordingly the perturbation energy ς_{CD} is equal to

$$\varsigma_{CD} = -(2/25)Z \quad \text{at} \quad v = 42/25 \tag{22}$$

The pair AB can transfer to all the empty orbitals of up-spin and then the number of allowed transitions is eight per unit length. Therefore the perturbation energy ς_{AB} is

$$\varsigma_{AB} = -(8/25)Z \quad \text{at} \quad v = 42/25 \tag{23}$$

The other pairs have the perturbation energies as

$$\varsigma_{EF} = \varsigma_{KL} = -(4/25)Z, \quad \varsigma_{GH} = \varsigma_{IJ} = -(6/25)Z, \quad \varsigma_{MN} = -(2/25)Z, \quad \varsigma_{OP} = \varsigma_{PQ} = 0 \quad \text{at} \quad v = 42/25 \tag{24}$$

The sum of the nearest electron pairs with up-spin is

$$F = \varsigma_{AB} + \varsigma_{CD} + \varsigma_{EF} + \varsigma_{GH} + \varsigma_{IJ} + \varsigma_{KL} + \varsigma_{MN} + \varsigma_{OP} + \varsigma_{PQ} = -(32/25)Z \tag{25}$$

The number of electrons with up-spin is seventeen in a unit sequence. Therefore the nearest pair energy per up-spin electron is

$$\varepsilon_{\uparrow} = -(32/(25 \times 17))Z \quad \text{at} \quad v = 42/26 \tag{26}$$

When the filling factor v is $(10s+2)/(6s+1)$ (s is a positive integer), the sum of the nearest-pair-energies inside the unit sequence is

$$F = -Z(2 + \cdots + (2s-2) + 2s + (2s-2) + \cdots + 2)/(6s+1) = -(2s^2/(6s+1))Z \tag{27}$$

The filling factor $(10s+2)/(6s+1)$ is larger than 5/3. The number of up-spin-electrons inside a unit length is equal to $(4s+1)$ and therefore the pair energy per up-spin-electron is given by

$$\varepsilon_{\uparrow} = -(2s^2/(6s+1)(4s+1))Z \quad \text{at} \quad v = (10s+2)/(6s+1) \tag{28}$$

When s becomes infinitely large, $\varepsilon_{\uparrow}$ approaches

$$\lim_{v \to (5/3)+0} \varepsilon_{\uparrow} = -(1/12)Z \tag{29}$$

Next we consider the filing factor 38/23 which is smaller than 5/3. The most uniform configuration is illustrated in **Figure 6**.

In this case, the sum of the nearest-pair-energies inside the unit sequence is

$$F = \varsigma_{AB} + \varsigma_{CD} + \varsigma_{EF} + \varsigma_{GH} + \varsigma_{IJ} + \varsigma_{KL} + \varsigma_{MN} = -(32/23)Z \tag{30}$$

At $v = (10s-2)/(6s-1)$, the sum of the nearest-pair-energies inside the unit sequence is

$$F = -\left[(2 + \cdots + (2s-2) + 2s + (2s-2) + \cdots + 2)/(6s-1)\right]Z = -(2s^2/(6s-1))Z \tag{31}$$
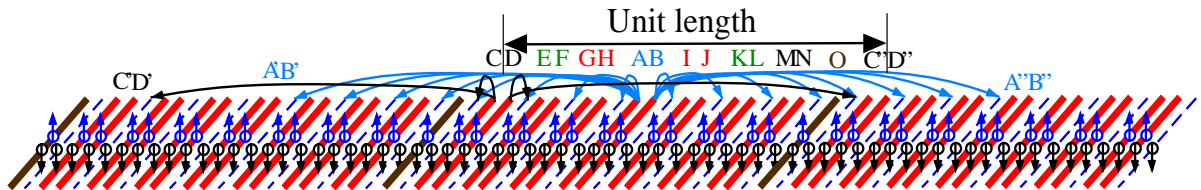
Accordingly

Figure 6. Electron configuration at $v = 38/23$.

$$\varepsilon_\uparrow = -\left(2s^2/(6s-1)(4s-1)\right)Z \quad \text{at} \quad v = (10s-2)/(6s-1) \tag{32}$$

$$\lim_{v \to (5/3)-0} \varepsilon_\uparrow = -(1/12)Z \tag{33}$$

Thus the energy gap appears between the energy value at $v = 5/3$ and the limiting value from the left and right sides:

$$\varepsilon_\uparrow(v = 5/3) - \lim_{v \to (5/3)\pm 0} \varepsilon_\uparrow = -(1/6)Z + (1/12)Z = -(1/12)Z \tag{34}$$

At the filling factor $v = (4j+1)/(2j+1)$, the energy gaps are listed in the fourth column of **Table 1**.

We consider the other cases. **Figure 7** shows the most uniform configuration of electrons at the filling factor $v = 8/5$. The x-, y-, z-directions are indicated at the upper-left of **Figure 7**.

The unit configuration is composed of five Landau orbitals and three electrons with up-spin. The number of the allowed transitions is two per unit length. Accordingly the perturbation energy ς_{AB} of the pair AB is expressed by Z as

$$\varsigma_{AB} = -(2/5)Z \quad \text{at} \quad v = 8/5 \tag{35}$$

The total number of the nearest electron pairs with up-spin is $1/3$ times $N_\uparrow$. Therefore the nearest pair energy per up-spin-electron is

$$\varepsilon_\uparrow = \left(\varsigma_{AB} \times \frac{1}{3}N_\uparrow\right)\Big/ N_\uparrow = -(2/15)Z \quad \text{at} \quad v = 8/5 \tag{36}$$

When the filling factor deviates from $v = 8/5$, the number of the Coulomb transitions decreases abruptly because the electron configuration at $v \neq 8/5$ disturbs the Coulomb transitions. As an example, the $v = 43/27$ state is illustrated in **Figure 8**.

Table 1. Energy gaps for $v = (4j+1)/(2j+1)$.

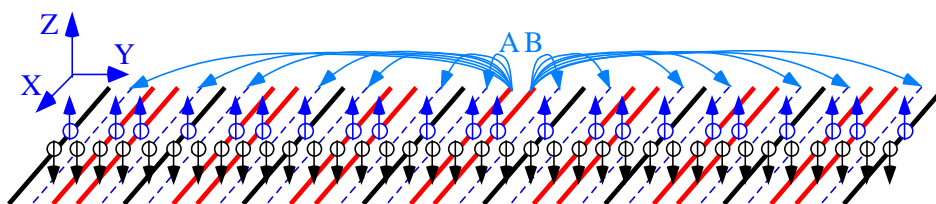| v_0	$\varepsilon_\uparrow(v_0)$	$\lim_{v \to v_0 \pm 0} \varepsilon_\uparrow(v)$	$\varepsilon_\uparrow(v_0) - \lim_{v \to v_0 \pm 0} \varepsilon_\uparrow(v)$
5/3	−(1/6) Z	−(1/12) Z	−(1/12) Z
9/5	−(1/20) Z	−(1/40) Z	−(1/40) Z
13/7	−(1/42) Z	−(1/84) Z	−(1/84) Z
17/9	−(1/72) Z	−(1/144) Z	−(1/144) Z

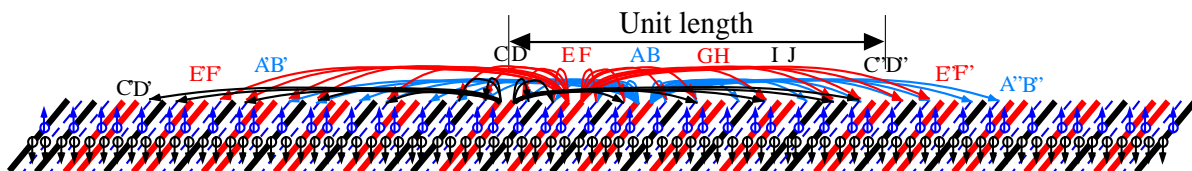
Figure 7. Electron configuration at $v = 8/5$.

Figure 8. Electron configuration at $v = 43/27$.

There are five up-spin-electron pairs placed in the nearest orbitals inside a unit length as in **Figure 8**. The number of allowed transitions is eleven for the pair AB, nine for EF and seven for CD in a unit length. Therefore the perturbation energies are obtained as follows:

$$\varsigma_{AB} = -(11/27)Z, \quad \varsigma_{EF} = \varsigma_{GH} = -(9/27)Z, \quad \varsigma_{CD} = \varsigma_{IJ} = -(7/27)Z \tag{37}$$

The sum of these pair energies is

$$F = \varsigma_{AB} + \varsigma_{CD} + \varsigma_{EF} + \varsigma_{GH} + \varsigma_{IJ} = -(43/27)Z \tag{38}$$

The number of electrons with up-spin is sixteen in a unit length and then the nearest pair energy per up-spin-electron is

$$\varepsilon_\uparrow = F/16 = -(43/(27 \times 16))Z \quad \text{at} \quad \nu = 43/27 \tag{39}$$

We examine more general cases of $\nu = (16s-5)/(10s-3)$. In the filling factor, the sum of the nearest-pair-energies inside a unit length is

$$F = -Z\big((2s+1) + (2s+3) + \cdots + (4s-1) + (4s-3) + \cdots + (2s+1)\big)/(10s-3)$$
$$= -\big((6s^2 - 4s + 1)/(10s-3)\big)Z \tag{40}$$

Accordingly

$$\varepsilon_\uparrow = -\big[(6s^2 - 4s + 1)/((10s-3)(6s-2))\big]Z \quad \text{at} \quad \nu = (16s-5)/(10s-3) \tag{41}$$

$$\lim_{\nu \to (8/5)-0} \varepsilon_\uparrow = -(1/10)Z \tag{42}$$

Next we study the FQH state with $\nu = 11/7$. The most uniform configuration is illustrated in **Figure 9**. The perturbation energy of the pair AB is

$$\varsigma_{AB} = -(3/7)Z \quad \text{at} \quad \nu = 11/7 \tag{43}$$

The number of the nearest electron pairs with up-spin is 1/4 of $N_\uparrow$. Therefore the nearest pair energy per up-spin-electron is

$$\varepsilon_\uparrow = \left(\varsigma_{AB} \times \frac{1}{4}N_\uparrow\right)\Big/N_\uparrow = -(3/28)Z \quad \text{at} \quad \nu = 11/7 \tag{44}$$

At $\nu = (3j-1)/(2j-1)$ the perturbation energy ς_{AB} for the nearest pair AB is obtained as

$$\varsigma_{AB} = -\big[(j-1)/(2j-1)\big]Z \quad \text{at} \quad \nu = (3j-1)/(2j-1) \tag{45}$$

The total number of the nearest electron pairs with up-spin is $1/j$ times $N_\uparrow$. Therefore the nearest pair energy per up-spin-electron is

$$\varepsilon_\uparrow = \left(\varsigma_{AB} \times \frac{1}{j}N_\uparrow\right)\Big/N_\uparrow = -\big[(j-1)/(j(2j-1))\big]Z \quad \text{at} \quad \nu = (3j-1)/(2j-1) \tag{46}$$
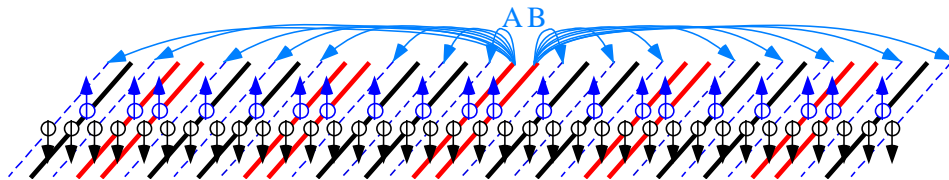

Figure 9. Electron configuration at $\nu = 11/7$.

The energies are listed in the second column of **Table 2**. Next we calculate the number of the allowed transitions in the neighbourhood of $v = (3j-1)/(2j-1)$. Then the energy gaps are shown in the fourth column of **Table 2**.

Thus the present theory yields the energy gaps at the specific filling factors as in **Table 1** and **Table 2**.

4. Electron Configurations and Energy Gaps for $1 < v < 3/2$

We examine the FQH states with $1 < v < 3/2$ in this section. Four examples are shown in **Figures 10-13** where the filling factors are $v = 4/3$, 6/5, 7/5 and 10/7, respectively. The electron configurations are illustrated in a 3D view where the down-spin electrons occupy all the Landau orbitals with the lowest level.

The most uniform electron configuration with up-spin is the repeat of the sequence (empty, filled, empty) at $v = 4/3$ as in **Figure 10**. The empty orbitals for up-spin are shown by red dashed lines and the filled orbitals

Table 2. Energy gaps for $v = (3j-1)/(2j-1)$.

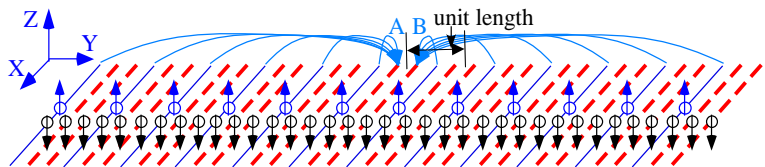| v_0	$\varepsilon_\uparrow(v_0)$	$\lim_{v \to v_0 \pm 0} \varepsilon_\uparrow(v)$	$\varepsilon_\uparrow(v_0) - \lim_{v \to v_0 \pm 0} \varepsilon_\uparrow(v)$
5/3	$-(1/6)Z$	$-(1/12)Z$	$-(1/12)Z$
8/5	$-(2/15)Z$	$-(1/10)Z$	$-(1/30)Z$
11/7	$-(3/28)Z$	$-(5/56)Z$	$-(1/56)Z$
14/9	$-(4/45)Z$	$-(7/90)Z$	$-(1/90)Z$

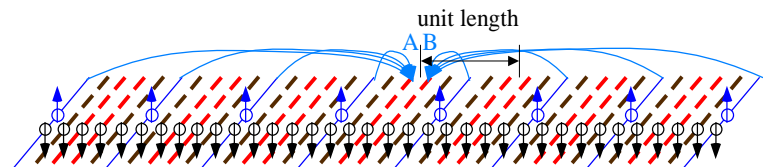**Figure 10.** Electron configuration at $v = 4/3$.

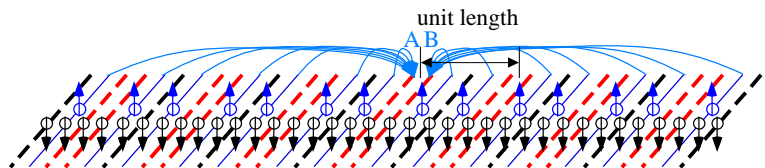**Figure 11.** Electron configuration at $v = 6/5$.

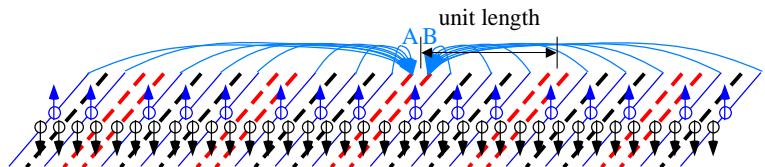**Figure 12.** Electron configuration at $v = 7/5$.

Figure 13. Electron configuration at $v = 10/7$.

with up-spin by blue lines. The blue arrows express the quantum transitions to the empty pairs AB. The symbol ς_{AB}^{H} means the perturbation energy via all the quantum transitions shown by blue arrow pairs. The nearest vacant-orbital-pair (nearest hole pair) AB is specified by the momenta p_A, p_B. The electron pair A'B' is also specified by the momenta p_A', p_B'. The electron pair A'B' transfers to the vacant orbitals at A and B. Therein the total momentum of the pair conserves in the Coulomb transition as

$$p_A' = p_A - \Delta p, \quad p_B' = p_B + \Delta p \tag{47}$$

where the momentum transfer Δp takes the following values as

$$\Delta p = (3j+1)2\pi\hbar/\ell \quad \text{for } j = 0, \pm 1, \pm 2, \pm 3, \cdots \tag{48}$$

at $v = 4/3$. Then the second order perturbation energy of the hole pair AB is given by

$$\varsigma_{AB}^{H} = \sum_{\Delta p = (3j+1)2\pi\hbar/\ell \text{ for } j=0,\pm1,\pm2,\cdots} \frac{\langle p_A', p_B' | H_I | p_A, p_B \rangle \langle p_A, p_B | H_I | p_A', p_B' \rangle}{W_G - W_{\text{excite}}(p_A' \to p_A, p_B' \to p_B)} \tag{49}$$

In order to evaluate the energy ς_{AB}^{H} we introduce the summation Z_H as

$$Z_H = - \sum_{\Delta p \neq 0, -2\pi\hbar/\ell} \frac{\langle p_A', p_B' | H_I | p_A, p_B \rangle \langle p_A, p_B | H_I | p_A', p_B' \rangle}{W_G - W_{\text{excite}}(p_A' \to p_A, p_B' \to p_B)} \tag{50}$$

where the momentum transfer Δp takes all the values $(2\pi\hbar/\ell) \times$ integer except $\Delta p = 0$ and $\Delta p = -2\pi\hbar/\ell$. The transferred state for $\Delta p = 0$ or $\Delta p = -2\pi\hbar/\ell$ is eliminated in the summation (50) because the diagonal element of H_I is absent. The denominator in Equation (50) is negative and so Z_H is positive. (The value of Z_H is nearly equal to Z for the same magnetic field strength.) The interval of momentum transfer is very small for a macroscopic size of a device and therefore the perturbation energy, ς_{AB}^{H}, can be expressed by Z_H as

$$\varsigma_{AB}^{H} = -\frac{1}{3} Z_H \quad \text{for} \quad v = 4/3 \tag{51}$$

The electron configurations at $v = 6/5$, 7/5 and 10/7 are illustrated in **Figures 11-13**, respectively. The perturbation energies, ς_{AB}^{H}, are also obtained by making use of Z_H as follows:

$$\varsigma_{AB}^{H} = -\frac{1}{5} Z_H \quad \text{for} \quad v = 6/5 \tag{52a}$$

$$\varsigma_{AB}^{H} = -\frac{2}{5} Z_H \quad \text{for} \quad v = 7/5 \tag{52b}$$

$$\varsigma_{AB}^{H} = -\frac{3}{7} Z_H \quad \text{for} \quad v = 10/7 \tag{52c}$$

In the unit length there are 1, 2, or 3 electrons for the filling factor $v = 6/5$, 7/5, or 10/7, respectively. Therefore the energy per electron becomes $-(1/5)Z_H$, $-(1/5)Z_H$ and $-(1/7)Z_H$. We express the perturbation energy per electron by the symbol $\varepsilon_\uparrow(v_0)$ at $v = v_0$ which is listed in the second column of **Table 3**.

The limiting values from both sides are calculated and written in the third column of **Table 3**. Subtractions of the limiting value from $\varepsilon_\uparrow(v_0)$ give the energy gaps which are listed in the fourth column of **Table 3**. **Tables 1-3** show the energy gaps at many filling factors. Thus the present theory can explain the confinement of the Hall resistance in the region of $1 < v < 2$.

5. Filling Factors with Even Integer for the Denominator

We examine the $v = 7/4$ state as an example with even integer for the denominator of the filling factor. **Figure 14** shows the most uniform configuration at $v = 7/4$.

There are many electron pairs in **Figure 14**. The pair AB is an example of the nearest electron pair. The

quantum transition via the Coulomb interaction conserves the total momentum. Accordingly the electron B should transfer to one orbital to the right when the electron A transfers to one orbital to the left. However the transformation to the right-direction is forbidden because the Landau orbital is already occupied by up-spin electron as shown by the blue arrows on **Figure 14**. When the electron A transfers to the fifth orbital to the left, the electron B cannot transfer to the fifth orbital to the right because of the Pauli exclusion principle. Thus all the transitions from the nearest electron pairs are forbidden via the Coulomb interaction. Therefore the electron pair AB has no binding energy. Also all the quantum transition from the electron pair BC are forbidden. Accordingly all the nearest electron pairs have no binding energy.

Similarly all the nearest electron pairs have no binding energy at the filling factor $v_0 = (4j-1)/(2j)$.

$$\varepsilon_\uparrow(v_0) = 0 \quad \text{at} \quad v_0 = (4j-1)/(2j) \tag{53}$$

The energies are listed in the second column of **Table 4**.

We examine the energies of the nearest electron pairs in the neighbourhood of $v = (4j-1)/(2j)$. As an example for the neighbourhood of $j = 2$, we have calculated the number of allowed transitions by using a computer, then we obtain

$$\varepsilon_\uparrow(v) = -\frac{5101}{121706} Z \quad \text{at} \quad v = 1 + \frac{302}{403} \tag{54a}$$

Table 3. Energy gaps for $v = (2j+2)/(2j+1)$ and $(3j+1)/(2j+1)$.

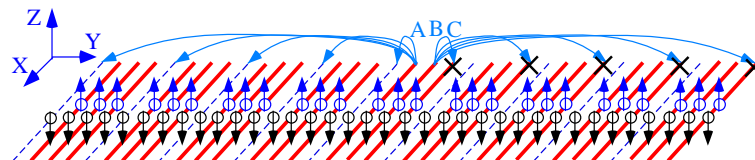| v_0	$\varepsilon_\uparrow(v_0)$	$\lim_{v \to v_0 \pm 0} \varepsilon_\uparrow(v)$	$\varepsilon_\uparrow(v_0) - \lim_{v \to v_0 \pm 0} \varepsilon_\uparrow(v)$
4/3	$-(1/3) Z_H$	$-(1/6) Z_H$	$-(1/6) Z_H$
6/5	$-(1/5) Z_H$	$-(1/10) Z_H$	$-(1/10) Z_H$
7/5	$-(1/5) Z_H$	$-(3/20) Z_H$	$-(1/20) Z_H$
8/7	$-(1/7) Z_H$	$-(1/14) Z_H$	$-(1/14) Z_H$
10/7	$-(1/7) Z_H$	$-(5/42) Z_H$	$-(1/42) Z_H$
10/9	$-(1/9) Z_H$	$-(1/18) Z_H$	$-(1/18) Z_H$
13/9	$-(1/9) Z_H$	$-(7/72) Z_H$	$-(1/72) Z_H$

Figure 14. Electron configuration at $v = 7/4$.

Table 4. Comparison of *nearest electron pair* energies at $v_0 = (4j-1)/(2j)$ and in its neighbourhood.

v_0	$\varepsilon_\uparrow(v_0)$	$\lim_{v \to v_0 \pm 0} \varepsilon_\uparrow(v)$	$\varepsilon_\uparrow(v_0) - \lim_{v \to v_0 \pm 0} \varepsilon_\uparrow(v)$
3/2	0	0	0
7/4	0	$-\dfrac{1}{24} Z$	$\dfrac{1}{24} Z$
11/6	0	$-\dfrac{1}{60} Z$	$\dfrac{1}{60} Z$
15/8	0	Negative	Positive

$$\varepsilon_\uparrow(v) = -\frac{501001}{12017006} Z \quad \text{at} \quad v = 1 + \frac{3002}{4003} \tag{54b}$$

$$\varepsilon_\uparrow(v) = -\frac{5101}{123120} Z \quad \text{at} \quad v = 1 + \frac{304}{405} \tag{54c}$$

$$\varepsilon_\uparrow(v) = -\frac{501001}{12031020} Z \quad \text{at} \quad v = 1 + \frac{3004}{4005} \tag{54d}$$

The limiting value of the pair energy for $v \to (3/4) \pm 0$ is obtained as follows:

$$\lim_{v \to 3/4 \pm 0} \varepsilon_\uparrow(v) = -\frac{1}{24} Z \tag{55}$$

Next we examine the case of $v_0 = 5/6$.

$$\varepsilon_\uparrow(v) = -\frac{5101}{304920} Z \quad \text{at} \quad v = 1 + \frac{504}{605} \tag{56a}$$

$$\varepsilon_\uparrow(v) = -\frac{501001}{30049020} Z \quad \text{at} \quad v = 1 + \frac{5004}{6005} \tag{56b}$$

$$\varepsilon_\uparrow(v) = -\frac{5101}{307142} Z \quad \text{at} \quad v = 1 + \frac{506}{607} \tag{56c}$$

$$\varepsilon_\uparrow(v) = -\frac{501001}{30071042} Z \quad \text{at} \quad v = 1 + \frac{5006}{6007} \tag{56d}$$

For the limiting of $v \to (5/6) \pm 0$ the nearest pair energy approaches

$$\lim_{v \to 5/6 \pm 0} \varepsilon_\uparrow(v) = -\frac{1}{60} Z \tag{57}$$

On the other hand the nearest pair energy at $v_0 = (4j-1)/(2j)$ is zero as obtained in Equation (53). Therefore the pair energy at $v_0 = (4j-1)/(2j)$ is higher than the energy in the neighbourhood of v_0. Then the peak values are listed in the fourth column of **Table 4**.

Similarly we calculate the quantum transition energy to the nearest empty orbitals at the filling factor $v = (2j+1)/(2j)$. The values are listed in **Table 5**.

Thus the FQH state is not stable at $v_0 = (4j-1)/(2j)$ and $v_0 = (2j+1)/(2j)$, because the energy is higher than that of the neighbourhood. That is to say, the Hall resistance confinement doesn't appear at $v_0 = (4j-1)/(2j)$ and $v_0 = (2j+1)/(2j)$. This theoretical result is in agreement with the experimental data.

6. Discussions

We have investigated the FQH states on the bases of the electromagnetic theory and the quantum theory without

Table 5. Comparison of *nearest electron pair* energies at $v = (2j+1)/(2j)$ and in its neighbourhood.

v_0	$\varepsilon_\uparrow(v_0)$	$\lim_{v \to v_0 \pm 0} \varepsilon_\uparrow(v)$	$\varepsilon_\uparrow(v_0) - \lim_{v \to v_0 \pm 0} \varepsilon_\uparrow(v)$
3/2	0	0	0
5/4	0	$-\frac{1}{8} Z_H$	$\frac{1}{8} Z_H$
7/6	0	$-\frac{1}{12} Z_H$	$\frac{1}{12} Z_H$
9/8	0	Negative	Positive

any quasi-particle. There are the other famous theories explaining the FQHE which are the Haldane-Halperin hierarchy theory and the composite fermion theory. Recently J.K. Jain has examined the distinct difference between them [31]. Also he summarized the composite fermion theory. The composite fermion theory deals with FQH states by dividing into several types as follows: We study the composite fermion theory for the electron filling-factors with the denominator smaller than 6 namely $v = 1/3$, 2/3, 4/3, 5/3, 1/5, 2/5, 3/5, 4/5, 6/5, 7/5, 8/5 and 9/5. These FQH states have the following structures as mentioned in the reference [31].

(1) $v = n/(2n+1) \rightarrow v = 1/3, 2/5, \cdots$

IQH state of composite fermion (which is an **electron** bound by **two** flux quanta)

(2) $v = n/(2n-1) \rightarrow v = 2/3, 3/5, \cdots$

IQH state of composite fermion (which is an **electron** bound by **two** flux quanta)

The effective magnetic field direction is **opposite** against the applied field.

(3) $v = n/(4n+1) \rightarrow v = 1/5, \cdots$

IQH state of composite fermion (which is an **electron** bound by **four** flux quanta)

(4) $v = 1 - n/(4n+1) \rightarrow v = 4/5, \cdots$

Combination state of the $v = 1$ electron IQH state and the IQH state of composite fermion (which is a **hole** bound by **four** flux quanta)

(5) $v = 1 + n/(4n+1) \rightarrow v = 6/5, \cdots$

Combination state of the $v = 1$ electron IQH state and the IQH state of composite fermion (which is an **electron** bound by **four** flux quanta)

(6) $v = 2 - n/(2n+1) \rightarrow v = 5/3, 8/5, \cdots$

Combination state of the $v = 2$ electron IQH state and the IQH state of composite fermion (which is a **hole** bound by **two** flux quanta)

(7) $v = 2 - n/(2n-1) \rightarrow v = 4/3, 7/5, \cdots$

Combination state of the $v = 2$ electron IQH state and the IQH state of composite fermion (which is a **hole** bound by **two** flux quanta)

The effective magnetic field direction is **opposite** against the applied field.

(8) $v = 2 - n/(4n+1) \rightarrow v = 9/5, \cdots$

Combination state of the $v = 2$ electron IQH state and the IQH state of composite fermion (which is a **hole** bound by **four** flux quanta)

We examine the composite fermion states for the five examples with $v = 4/3$, $v = 5/3$, $v = 6/5$, $v = 9/5$ and $v = 4/5$.

1) FQH state at $v = 4/3$

In the article [31] the $v = 4/3$ FQH state is constructed by combining the $v = 2$ IQH state with the composite fermion state of hole for $v = -2/3$ as in **Figure 15**. Therein the black dots on the green sheet indicate the electrons in the $v = 2$ IQH state. The composite fermions of hole are expressed by the white circles on the yellow sheet, each of which is bound with two flux quanta as in **Figure 15**.

The effective magnetic field is expressed by the red arrows, the direction of which is opposite against the applied magnetic field. The total filling factor is the sum of $v = 2$ and $v = -2/3$. Accordingly the filling factor of electrons becomes $v = 4/3$.

2) FQH state at $v = 5/3$

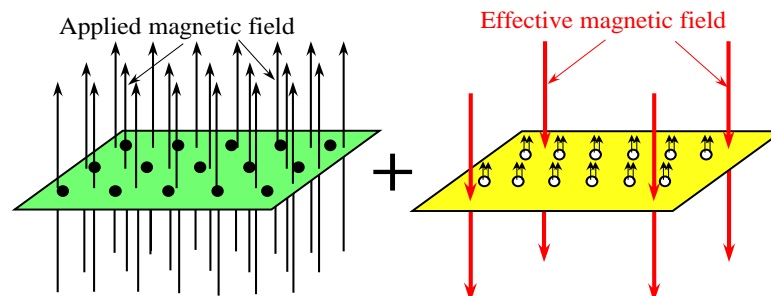The $v = 5/3$ FQH state is explained by the combination of the $v = 2$ IQH state and the composite fermion

Figure 15. Composite fermion theory for $v = 4/3$.

state of hole with $v = -1/3$. Each hole is bound with two flux quanta and the effective magnetic field is parallel to the applied magnetic field as shown in **Figure 16**.

3) FQH state at $v = 6/5$

The $v = 6/5$ FQH state is produced by combining the $v = 1$ IQH state with the composite fermion state with $v = 1/5$. Therein the electron of the $v = 1$ IQH state is expressed by the black circles on the sky-blue sheet in **Figure 17**. The residual electrons are expressed by the blue dots on the pink sheet, each of which is bound by the four flux quanta as seen in **Figure 17** schematically. That is to say, some electrons are unbound with magnetic flux quanta and the other electrons are bound with flux quanta. However all the electrons exist in the same conducting thin layer and their wave functions are overlapping with each other. Furthermore in the many-body problem all the wave functions of electrons should satisfy the anti-symmetric relation. Also all the electrons should be affected by the same magnetic field. Accordingly the combination of the $v = 1$ IQH state and the $v = 1/5$ composite fermion state has some difficulty.

4) FQH state at $v = 9/5$

The $v = 9/5$ FQH state is created by combining the $v = 2$ IQH state with the composite fermion state of hole for $v = -1/5$ as illustrated in **Figure 18**.

Therein the black dots on the green sheet indicate the electrons in the $v = 2$ IQH state. The composite fermions of hole are expressed by the white circles on the yellow sheet, each of which is bound with four flux quanta as seen in **Figure 18**.
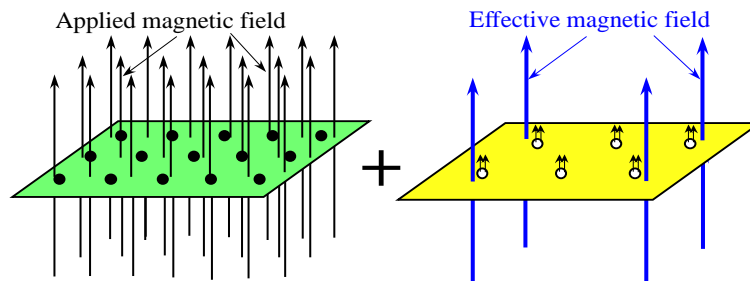

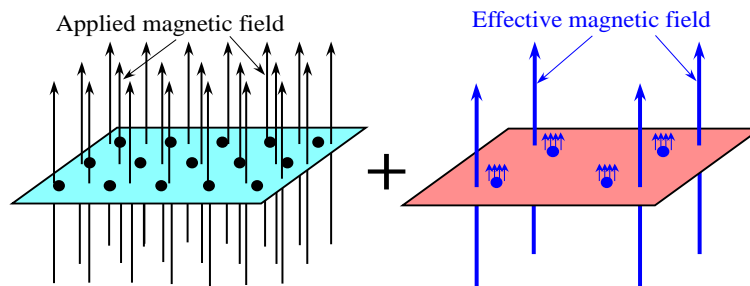**Figure 16.** Composite fermion theory for $v = 5/3$.

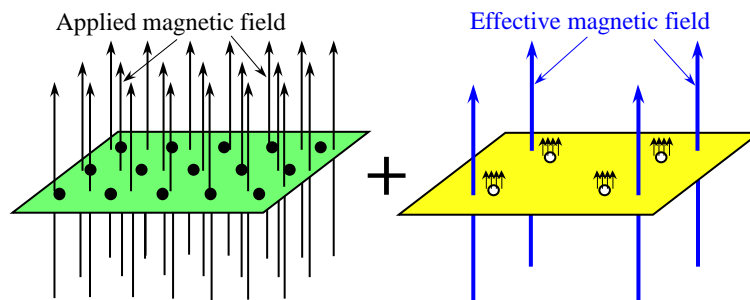**Figure 17.** Composite fermion theory for $v = 6/5$.

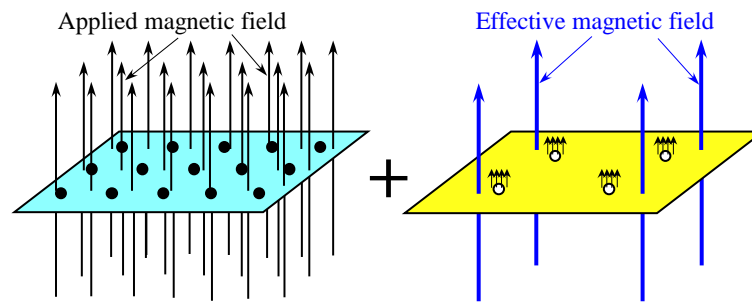**Figure 18.** Composite fermion theory for $v = 9/5$.

Figure 19. Composite fermion theory for $\nu = 4/5$.

5) FQH state at $\nu = 4/5$

The $\nu = 4/5$ FQH state is produced by combining the $\nu = 1$ IQH state with the composite fermion state of hole with $\nu = -1/5$. Therein the electron of the $\nu = 1$ IQH state is expressed by the black circles on the sky-blue sheet in **Figure 19**. The composite fermions of hole are expressed by the white circles on the yellow sheet, each of which is bound by the four flux quanta.

Thus the composite fermion theory uses many different kinds of quasi-particles and different directions of the effective magnetic field. When the filling factor varies by adjusting the gate voltage (or the applied magnetic field strength), the quasi-particle changes from hole to electron, the number of the bound flux-quanta changes, and the direction of the effective magnetic field changes from parallel to anti-parallel. These complicated assumptions are too artificial.

The quantum Hall system is originally described by the same Hamiltonian for all the filling factors. Therefore it is necessary that the FQHE is derived only from the original Hamiltonian by using the normal electrons and the usual quantum physics without any quasi-particle. This article succeeds to explain the FQHE which is produced by the abrupt change of the quantum-transition number. The abrupt change is caused by the momentum conservation, the most uniform configuration of electrons and the Fermi statistics.

7. Summary

The Hall resistance confinement is observed in the measurement of the current and the Hall voltage. In the real experiment, the Hall voltage is extremely large in comparison with the potential voltage. The ratio of (Hal voltage)/(potential voltage) is larger than 10^9 for the IQHE. Also the ratio is very large for the FQHE. That is to say, we cannot ignore the electric potential gradient in the direction of Hall voltage. Almost all the theories of FQHE neglect this electric potential gradient and use the symmetric property for the x- and y-directions on the 2D-electron plain. We have examined the eigen-states of single electron under the electric potential with the gradient. Then we have obtained the most uniform configuration of electrons in the Landau orbitals, the states of which satisfy the eigen-equation of the Hamiltonian (8). The Coulomb interaction produces the quantum transitions of electron pair (not single electron), because the interaction acts between two electrons. Therefore the total momentum along the current direction conserves between before and after transitions. Fermi statistics of electrons create abrupt change in the number of the allowed transitions for varying of the filling factor. This abrupt change produces an energy gap which yields the confinement of the Hall resistance at the specific fractional filling factors. This article and the previous works have clarified these mechanisms. The results are in a good agreement with the experimental data.

Acknowledgements

References

[1]   Jain, J.K. (2007) Composite Fermions. Cambridge University Press, New York.

http://dx.doi.org/10.1017/CBO9780511607561

[2] Das Sarma, S. (1996) Localization, Metal-Insulator Transitions, and Quantum Hall Effect. In: Das Sarma, S. and Pinczuk, A., *Perspectives in Quantum Hall Effects*: *Novel Quantum Liquids in Low-Dimensional Semiconductor Structures*, Wiley, New York, 1-36. http://dx.doi.org/10.1002/9783527617258.ch1

[3] Jain, J.K. and Kamilla, R.K. (1998) Composite Fermions: Particles of the Lowest Landau Level. In: Heinonen, O., Ed., *Composite Fermions*: *A Unified View of the Quantum Hall Regime*, World Scientific, New York, 1-90. http://dx.doi.org/10.1142/9789812815989_0001

[4] Jain, J.K. (1989) *Physical Review Letters*, **63**, 199-202. http://dx.doi.org/10.1103/PhysRevLett.63.199

[5] Kamilla, R.K., Wu, X.G. and Jain, J.K. (1996) *Physical Review Letters*, **76**, 1332. http://dx.doi.org/10.1103/PhysRevLett.76.1332

[6] Jain, J.K. and Kamilla, R.K. (1997) *Physical Review B*, **55**, R4895. http://dx.doi.org/10.1103/PhysRevB.55.R4895

[7] Park, K. and Jain, J.K. (1998) *Physical Review Letters*, **80**, 4237. http://dx.doi.org/10.1103/PhysRevLett.80.4237

[8] Stormer, H.L. and Tsui, D.C. (2007) Composite Fermions in the Fractional Quantum Hall Effect. In: Das Sarma, S. and Pinczuk, A., Eds., *Perspectives in Quantum Hall Effects*: *Novel Quantum Liquids in Low-Dimensional Semiconductor Structures*, Wiley, New York, 385-421. http://dx.doi.org/10.1002/9783527617258

[9] Jain, J.K. (2000) *Physics Today*, **53**, 39. http://dx.doi.org/10.1063/1.883035

[10] Halperin, B.I. (2003) *Physica E*: *Low-Dimensional Systems and Nanostructures*, **20**, 71-78. http://dx.doi.org/10.1016/j.physe.2003.09.022

[11] Murthy, G. and Shankar, R. (2003) *Reviews of Modern Physics*, **75**, 1101-1158. http://dx.doi.org/10.1103/RevModPhys.75.1101

[12] Sitko, P., Yi, K.-S. and Quinn, J.J. (1997) *Physical Review B*, **56**, 12417-12421. http://dx.doi.org/10.1103/PhysRevB.56.12417

[13] Tao, R. and Thouless, D.J. (1983) *Physical Review B*, **28**, 1142-1144. http://dx.doi.org/10.1103/PhysRevB.28.1142

[14] Tao, R. (1984) *Physical Review B*, **29**, 636-644. http://dx.doi.org/10.1103/PhysRevB.29.636

[15] Sasaki, S. (2011) Binding Energy, Polarization of Fractional Quantum Hall State. *Proceedings of the* 25*th International Conference on the Physics of Semiconductors*, Osaka, 17-22 September 2000, 925-926.

[16] Sasaki, S. (2003) *Surface Science*, **532-535**, 567-575. http://dx.doi.org/10.1016/S0039-6028(03)00091-8

[17] Sasaki, S. (2004) *Surface Science*, **566-568**, 1040-1046. http://dx.doi.org/10.1016/j.susc.2004.06.101

[18] Sasaki, S. (2005) Binding Energies and Spin Polarizations of Fractional Quantum Hall States. In: Norris, C.P., Ed., *Surface Science*: *New Research*, Nova Science Publishers, Hauppauge, 103-161.

[19] Sasaki, S. (2013) *ISRN Condensed Matter Physics*, **2013**, Article ID: 489519. http://dx.doi.org/10.1155/2013/489519

[20] Sasaki, S. (2012) *Advances in Condensed Matter Physics*, **2012**, Article ID: 281371. http://dx.doi.org/10.1155/2012/281371

[21] Sasaki, S. (2014) *ISRN Condensed Matter Physics*, **2014**, Article ID: 468130.

[22] Sasaki, S. (2000) *Physica B*: *Condensed Matter*, **281-282**, 838-839. http://dx.doi.org/10.1016/S0921-4526(99)00840-6

[23] Sasaki, S. (2008) *Journal of Physics*: *Conference Series*, **100**, Article ID: 042021. http://dx.doi.org/10.1088/1742-6596/100/4/042021

[24] Sasaki, S. (2008) *Journal of Physics*: *Conference Series*, **100**, Article ID: 042022.

[25] Sasaki, S. (2010) *E-Journal of Surface Science and Nanotechnology*, **8**, 121-124. http://dx.doi.org/10.1380/ejssnt.2010.121

[26] Sasaki, S. (2013) *Journal of Modern Physics*, **4**, 1-7. http://dx.doi.org/10.4236/jmp.2013.49A001

[27] Sasaki, S. (2007) Calculation of Binding Energies for Fractional Quantum Hall States with Even Denominators. http://arxiv.org/abs/cond-mat/0703360

[28] Sasaki, S. (2007) Energy Spectra for Fractional Quantum Hall States. http://arxiv.org/abs/0708.1541

[29] Sasaki, S. (2008) Consideration of ac Josephson Effect in Fractional Quantum Hall States. http://arxiv.org/abs/0807.0288

[30] Sasaki, S. (2008) Frequency Dependence of Diagonal Resistance in Fractional Quantum Hall Effect via Periodic Modulation of Magnetic Field. http://arxiv.org/abs/0803.0615

[31] Jain, J.K. (2014) *Indian Journal of Physics*, **88**, 915-929. http://dx.doi.org/10.1007/s12648-014-0491-9